STIFFNESS OF GLYCERINATED RABBIT PSOAS FIBERS IN THE RIGOR STATE

Filament-Overlap Relation

KATSUHISA TAWADA AND MICHIO KIMURA
Department of Biology, Faculty of Science, Kyushu University, Fukuoka 812, Japan

ABSTRACT The stiffness of glycerinated rabbit psoas fibers in the rigor state was measured at various sarcomere lengths in order to determine the distribution of the sarcomere compliance between the cross-bridge and other structures. The stiffness was determined by measuring the tension increment at one end of a fiber segment while stretching the other end of the fiber. The contribution of the end compliance to the rigor segments was checked both by laser diffractometry of the sarcomere length change and by measuring the length dependence of the Young's modulus; the contribution was found to be small. The stiffness in the rigor state was constant at sarcomere lengths of 2.4 μm or less; at greater sarcomere lengths the stiffness, when corrected for the contribution of resting stiffness, scaled with the amount of overlap between the thick and thin filaments. These results suggest that the source of the sarcomere compliance of the rigor fiber at the full overlapping of filaments is mostly the cross-bridge compliance.

INTRODUCTION

The interaction of the myosin cross-bridge with the actin accompanying ATP splitting is the key reaction for tension generation in muscle (H. E. Huxley, 1969; A. F. Huxley, 1974; Eisenberg and Hill, 1978). To explore the mechanical aspects of the interaction (Huxley, 1957; Civan and Podolsky, 1966), Huxley and Simmons (1970, 1971) analyzed the isometric tension transient, which is produced by active muscle when the muscle fiber is released or stretched quickly. The first response in the transient is the elastic tension decrease or increase during the release or stretch of the fiber, which is followed by dynamic tension recovery to the original level. To account for the transients, Huxley and Simmons (1971) developed a "cross-bridge rocking" model. The model assumed that the rocking of the cross-bridge on the thin filament results in the stretching of a series elastic element, which in turn provides the force of the sliding between the thick and thin filaments. They tentatively located the elastic element in the SII portion of the cross-bridge in their model. Later work showed that most of the compliance of active muscle is in the cross-bridge (Ford et al., 1977, 1981).

As Huxley (1974) pointed out, the structure and the nature of the cross-bridge compliance are not yet known. With the final aim of elucidating them, we studied the stiffness of fibers in the rigor state because it is much easier to measure the rigor stiffness than to measure the "instantaneous" stiffness of active fibers. Because the distribution of sarcomere compliance between cross-bridges and other structures in rigor fibers is not known, we set out to measure it, as it appears to be important. Glycerinated rabbit psoas fibers were used in the study. The stiffness was determined by measuring the tension increment at one end of a fiber segment of muscle while stretching the other end of the fiber. In this article we will show that most of the sarcomere compliance of rigor fibers originates in the cross-bridge. A preliminary account of the work has been reported (Tawada and Kimura, 1983).

MATERIALS AND METHODS

Fiber Preparation

Glycerinated rabbit psoas fibers were prepared by the following two methods. In the first method, rabbit psoas fibers were initially glycerinated at 4°C for 24 h in a 50% mixture of glycerol and a solution containing 5 mM phosphate buffer of pH 6.8 and 10 mM EGTA. After the glycerination, the fibers were transferred into another 50% mixture of glycerol and a solution containing 100 mM KCl, 10 mM EGTA, 5 mM $MgCl_2$, and 10 mM phosphate buffer of pH 6.8, and stored at −20°C. This preparation will be referred to as fibers glycerinated in the rigor state. In the second method, rabbit psoas fibers were initially "chemically skinned" in a relaxing solution (150 mM K propionate, 5 mM EGTA, 5 mM phosphate buffer of pH 6.8, 3mM Mg acetate, 3 mM ATP) at 0°C according to the method of Eastwood et al. (1979). After the skinning for 24 h, the fibers were transferred into a 50% mixture of glycerol and the same relaxing solution, and stored at −20°C. This preparation will be referred to as fibers glycerinated in the relaxed state. Fresh skinned fibers (before glycerination) were sometimes used for experiments. Glycerinated fibers were used within 3 mo of preparation.

Apparatus and Procedure

Fig. 1 shows a schematic diagram of the apparatus. Generally, it was very similar to that described by Gulati and Podolsky (1978), except that a

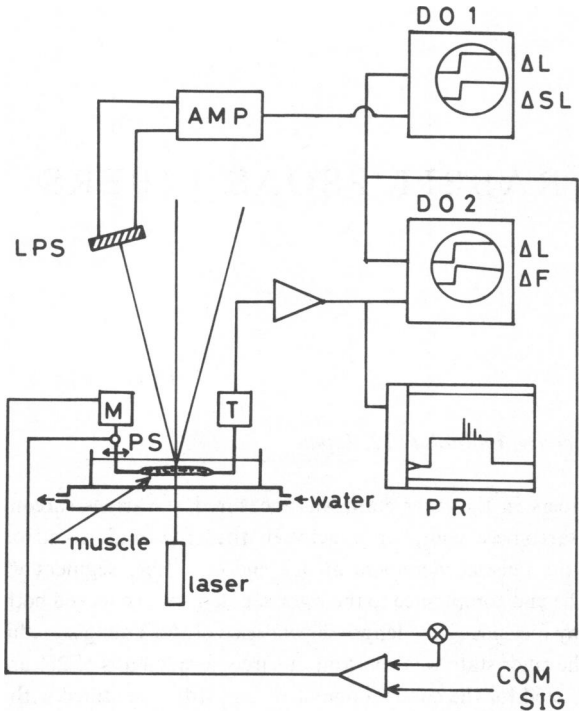

FIGURE 1 Schematic diagram of the experimental setup used for stiffness measurements. *M*, servo motor; *T*, force transducer; *LPS*, light position sensor; *DO 1* and *2*, digital oscilloscopes (Nicolet Explorer II, Nicolet Instrument Corp., Madison, WI); ΔL, length displacement; ΔSL, sarcomere length change detected by *LPS*; ΔF, tension response by muscle; *PR*, pen recorder for long time-measurements of tension; *COM SIG*; command signal from a pulse generator.

servomotor with a displacement sensor was used instead of a displacement transducer and diffraction from a helium-neon gas laser (Nippon Electric Co., Ltd., Tokyo, GLG5220, beam size = 0.8 mm, λ = 632.8 nm) was used to monitor the change in the sarcomere length of muscle segments.

Force Transducer. A Norway force transducer (AE 801, Aksjeselskapet Mikroelectronikk, Horten, Norway) was used for the measurement of tension in the fiber. A short attachment wire (0.1 × 4 mm, stainless steel) was cemented to the end of the beam of the transducer and used for mounting a muscle fiber segment. The natural frequency of transducer was 6.3 kHz in the air and 3.3 kHz in water.

Servomotor. Initially, we used a homemade servo system, which was made of a voice coil of a speaker, as described by Delay et al. (1979). The servo system was driven by a DC servoamplifier with a feedback system. The linear compliance of the servo system at the tip with feedback was 0.5 μm/g.

We later used an optical scanner (G-100PD, General Scanning Inc., Watertown, MA) as a servomotor. The CCX-100 servo controller (General Scanning Inc.) was used for the positional control of the scanner. One end of an arm made of magnesium ribbon (22 × 2 ×0.24 mm), which was made stiff by being coated with glue, was attached to the shaft of the scanner motor. A short attachment wire cemented to the other end of the arm was used for mounting a muscle segment. The compliance of the arm at the tip was 3 μm/g.

Command signals from a pulse generator were fed into the servoamplifier or into the scanner controller for changing the length of muscle segment. The step time for the length change was set to 3 ms in the present experiment to circumvent difficulties due to mechanical oscillation of the motor arm and the transducer beam.

Laser Diffractometry. To detect small changes in sarcomere length, the first-order diffraction line of laser light from a muscle segment was focused on a light position sensor (United Detector Technology Inc., Santa Monica, CA, SC-10) by a cylindrical lens. The difference in signal from the two terminals of the detector was proportional to the position of the centroid of the light of a diffraction line and proportional also to the light intensity. Thus, the signal difference was electrically divided by the sum of the signals from both terminals, so that the normalized signal was independent of the light intensity. The detector was calibrated for each experiment by a known movement of the detector. The normalized signal was converted into the change in sarcomere length with a programmable calculator.

General Procedure. Segments of a single fiber or a small bundle of fibers were dissected out from glycerinated fibers in 50% glycerol solution. Fibers glycerinated in the rigor state were dissected out in the 50% glycerol (rigor) solution. Fibers glycerinated in the relaxed state were dissected out in the 50% glycerol (relaxing) solution. Sometimes segments of a single fiber were dissected out from fresh "chemically skinned" fibers, which were not yet glycerinated, in the skinning solution.

One end of a fiber segment was tied to the force transducer, and the other end, to the servomotor, with surgical silk (No. 6-0, Nescosuture Lab., Osaka, Japan) under a microscope. The tying was carried out in the same solution used for dissection. Then the fiber segment was transferred into relaxing solution (or sometimes into rigor solution) for rinsing. All these procedures were carried out at low temperatures below 10°C unless otherwise stated.

Solutions

Rigor Solution. 80 mM KCl, 40 mM imidazole (pH 7.0 at 0 C), 5 mM EDTA.

Relaxing Solution. 80 mM KCl, 40 mM imidazole (pH 7.0 at 0°C), 5 mM Na_2ATP, 2 mM $MgCl_2$, 5 mM EGTA.

Contracting solution. 80 mM KCl, 40 mM imidazole (pH 7.0 at 0 C), 2 mM Na_2ATP, 1 mM $MgCl_2$, 5 mM (EGTA + CaEGTA) (pCa 5).

RESULTS

We determined the stiffness of glycerinated rabbit psoas fibers in the rigor (or in the relaxed) state by measuring the tension increment at one end of a fiber segment while giving a quick stretch to the other end of the fiber segment.

The tension and stiffness developed by a muscle when the muscle goes into rigor depends on the condition of the muscle before rigor, e.g., the composition of the solutions used. Kawai and Brandt (1976) showed that fibers entering rigor during maximum activation develop larger tension and larger stiffness than those induced into rigor with a minimum of activation. The dependence of the stiffness on the rigor tension could be due to incomplete removal of the slack in rigor fibers when the degree of activation was small, i.e., when the rigor tension was small. Therefore, we first studied how the rigor stiffness devel-

oped by muscle fibers depends on the stress imposed on the fibers, which was given either by the development of the rigor tension in the fibers or by the manual stretching of the fibers.

Fig. 2 shows the responses in tension of a fiber segment to stretching in rigor. The tension increment induced by the stretch decayed slowly with time. The rate of the tension decay depended on the amplitude of the stretch: the larger the amplitude, the faster the decay. The step time for stretch in our experiments was set to 3 ms.

Fig. 3 summarizes the relationship of the tension increment to the amplitude of stretch under different stresses. The muscle fiber used for obtaining the results in Fig. 3 was initially in relaxing solution and then transferred to rigor solution. A small rigor tension (≃0.1 kg/cm^2) developed. Observation of the fiber segment under a microscope showed that the slack of the fiber had not yet been

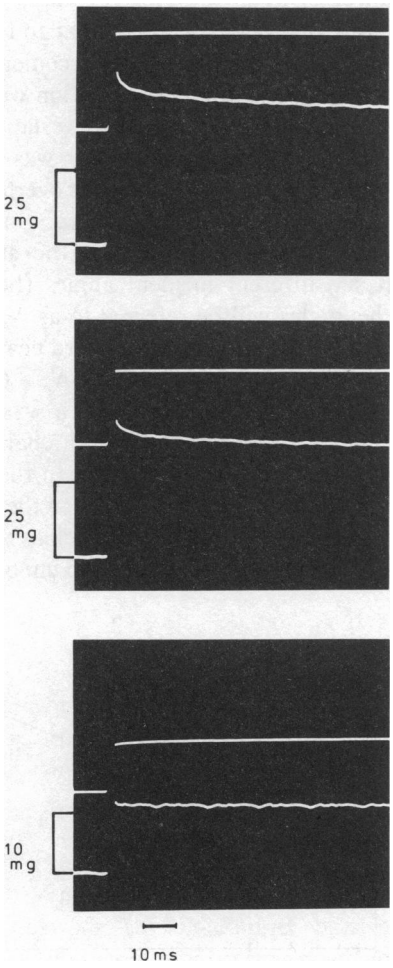

FIGURE 2 Tension changes due to stretch of a single-fiber segment in rigor. In each panel, the top trace shows the imposed length change and the bottom trace, the tension response. The imposed length changes given at one end of the fiber segment were 1.07% muscle length (*top* panel), 0.81% muscle length (*middle* panel), and 0.21% muscle length (*bottom* panel). Muscle segment length = 0.35 cm; sarcomere length = 2.55 μm. 13°C.

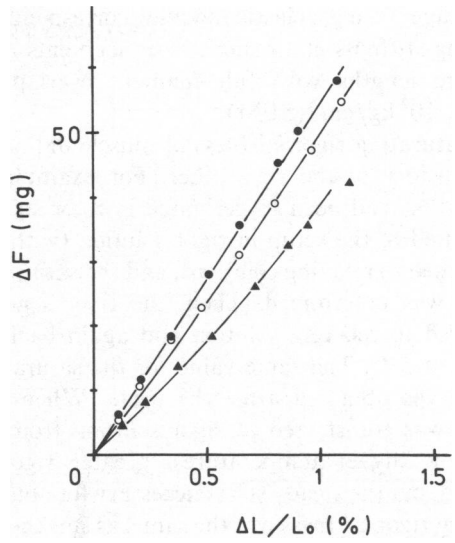

FIGURE 3 Tension increment vs. stretch-length relations of a segment of single fiber in rigor. Muscle segment length = 0.35 cm; sarcomere length = 2.55 μm; steady stress = 0.2 kg/cm^2 (▲); 0.4 kg/cm^2 (○); 0.5 kg/cm^2 (●).

completely taken out. After the development of the rigor tension, the fiber was manually stretched to impose more stress on the fiber. The tension produced by the manual stretching began to decay very slowly with time, and the decay almost stopped within ½ h. Then, a couple of short quick stretches of different amplitude were successively (with an interval of 1–2 min) applied to the fiber, and the initial values of the resulting tension increments were measured. To impose more stress, the fiber was manually stretched again and the stiffness was measured under a greater steady stress. The procedure was repeated. The sarcomere length of the fiber did not change appreciably when the steady stress was increased from about 0.1 kg/cm^2 to greater values.

When the steady stress was small, the relationship between tension increment and stretch amplitude was not linear and the stiffness was small. With the increase of the steady stress, the relationship of the tension increment to the amplitude became less curved and the stiffness became larger. Finally, when the steady stress was >0.5 kg/cm^2, the relationship became almost linear, the stiffness being insensitive to the magnitude of the stress. Observing the fiber under a microscope revealed that the slack seemed to be taken out of the fiber segment just when the steady stress was 0.5 kg/cm^2. The slope of the final linear plot (●) shows the saturating stiffness. Note that regardless of the initial stress, for large enough stretches, the slope of the tension increment–stretch amplitude relationships becomes linear and has a value equal to the saturating stiffness. A similar finding was made by Güth and Kuhn (1978; see their Fig. 6). The value of the steady stress necessary for obtaining the saturating stiffness varied from fiber segment to fiber segment but was ~0.3–0.6 kg/cm^2.

The average Young's elastic modulus corresponding to the saturating stiffness of 14 single fiber segments in rigor at sarcomere lengths with full filament overlap was 2.5 (± 0.1) $\times$ 10^2 kg/cm^2 (SEM).

The saturating rigor stiffness of muscle did not depend on the history of the rigor fiber. For example, a fiber segment that had been glycerinated in rigor solution was initially tied to the setup in rigor solution (without being ever exposed to relaxing solution), and the saturating rigor stiffness was determined. Then, the fiber segment was transferred to relaxing solution and again back to rigor solution, at 5°C. The same value for the saturating rigor stiffness was obtained after the cycle. When the fiber segment was transferred to rigor solution from relaxing solution at higher temperatures, greater rigor tension developed, but the steady stress necessary for obtaining the saturating rigor stiffness was the same, as was the stiffness. Because of the independence of the saturating rigor stiffness of a muscle from the condition of the muscle before measuring the rigor stiffness, we took the saturating rigor stiffness as the true stiffness of the rigor fiber. Hereafter, the saturating rigor stiffness will be simply referred to as the rigor stiffness.

The rigor stiffness remained the same when pH was varied from 7.0 to 7.4 or 8.5 in the presence of 80 mM KCl + 40 mM buffer (imidazole at pH 7.0 or 7.4, triethanolamine at pH 8.5) at 15°C. Reduction of ionic strength by lowering the KCl concentration from 80 to 5 mM did not affect the rigor stiffness.

The rigor stiffness did not change when the concentration of free Ca^{++} was varied from $\sim 10^{-9}$ to 10^{-3} M. Addition of free 1 mM Mg^{++} or removal of a trace amount of free Mg^{++} by EDTA did not affect the rigor stiffness.

There was no appreciable difference in the rigor stiffness between fresh skinned rabbit psoas fibers (before glycerination) and fibers glycerinated in the relaxed or in the rigor state at -20°C for 3 mo.

Small Contribution of End Compliance

The elastic property of muscle near the tying knots in a fiber segment (end compliance) may be different from the true elastic property of the muscle fiber. We checked the contribution of end compliance to the rigor stiffness measurement by studying the dependence of the Young's elastic modulus on the fiber segment length at full overlap and also by laser diffractometry of the sarcomere length change.

If there is no contribution of end compliance, the Young's elastic modulus of a fiber segment will not depend on the segment length, because the modulus is a parameter normalized with the length of a fiber segment. On the contrary, if there is a contribution of end compliance, the Young's modulus will depend on the muscle length. From the length dependence, we can evaluate the contribution of end compliance, as discussed in Appendix A.

For the analysis, we determined the Young's modulus of fiber segments in rigor, starting with segments of ~1 cm in length. Then, the length was reduced to $1/n$, e.g., ½, by cutting and reattaching and the Young's modulus of the shorter segments was determined. The ratio of the Young's modulus before the length reduction to that after the length reduction was plotted as a function of n, which is the ratio of the original length to the reduced length. By applying Eq. A4 given in Appendix A to the results summarized in Fig. 4, we obtained 0.925 for A in Eq. A4. This, together with Eq. A5 means that 92.5% of a length change applied at one end of a muscle segment (of ~1 cm in length) goes to the sarcomere at the middle portion of the fiber segment. Eq. A6 calculates that for a ½-cm muscle segment, 86% of a given length change goes to the central sarcomeres, and for a ⅓-cm segment, 80% of a given length change goes to the sarcomeres.

Laser diffractometry of sarcomere length change gave a similar value for the contribution of the end compliance (Fig. 5). However, when the incident angle of the laser beam was varied in a plane perpendicular to the long axis of the fiber ($\leq \pm 11°$), changes in the sarcomere length for a fixed stretch length varied. The variation was relatively large except at zero or small filament overlap. For example, when a stretch of 0.5% muscle length was given to one end of a fiber segment with full filament overlap (0.37 cm long at the sarcomere length of 2.4 μm) in rigor, and changes in the sarcomere length for the stretch were measured at six different incident angles (hereafter the number of the angles will be referred to as N_a), the average length change going to the sarcomere near the center of the fiber segment was 85 ± 13% (SD, $N_a = 6$), although the tension increment due to the stretch was nearly the same each time. Thus, the actual length change given at one end of the fiber segments, rather than the sarcomere length change, was taken as the strain for the determination of the stiffness in this study. Inasmuch as the length of fiber segments in our study was ~0.3–0.5 cm or longer, we

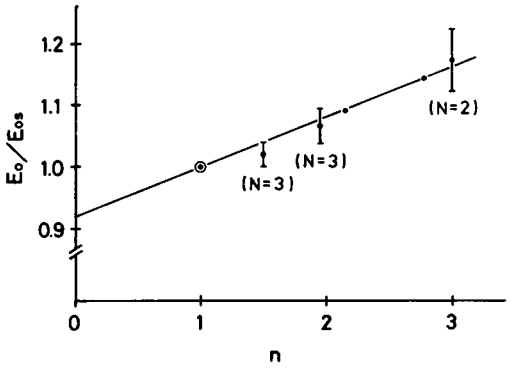

FIGURE 4 Dependence of the Young's modulus of rigor fibers on the length of the fiber segments. E_o, the initial Young's modulus of a fiber segment (~1 cm) at full overlap in rigor; E_{os}, the Young modulus of the fiber segment in rigor after its length reduction to $1/n$ of the original length. The error bars show the standard error of the mean. Points without error bar show single measurements.

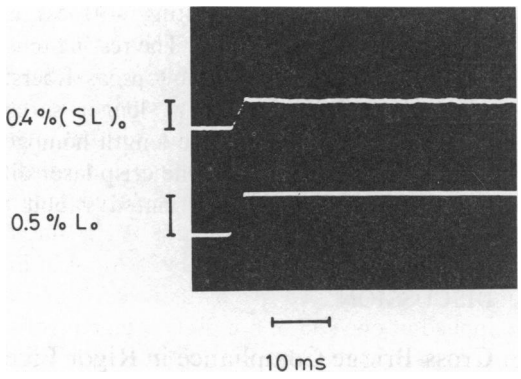

FIGURE 5 Response in sarcomere length (*upper* trace) to a length change given at one end of a bundle of rigor fibers. The upper trace actually shows a positional change of the first layer line of the laser beam from the center of the fiber bundle. Note the relaxation of sarcomere length due to an internal redistribution of sarcomere lengths which was also found by Brenner et al. (1982). The positional change was converted into a sarcomere length change by calculation (see Materials and Methods). Muscle segment length = 0.365 cm; sarcomere length = 2.43 μm. The bundle consisted of three single fibers.

found the contribution of end compliance in our study to be small.

The contribution of end compliance appears to be smaller in rigor fibers with smaller filament overlap. For example, the average length change going to the sarcomere, which was determined by the laser diffractometry, was 100 ± 2% (SD, N_a = 4) with a single fiber segment in rigor with zero filament overlap (0.36 cm long at the sarcomere length of 3.9 μm). At 50% filament overlap (a 0.44-cm-long muscle segment in rigor at the sarcomere length of 3.1 μm), the average relative length change was 92 ± 10% (SD, N_a = 8). The standard deviation, except at zero or small filament overlap, was too large for the laser diffractometry to provide a precise expression for the dependence of the relative length change on the filament overlap, or on the fiber segment length at a fixed filament overlap, in rigor fibers.

Dependence of Rigor Stiffness on the Sarcomere Length

To determine the distribution of sarcomere compliance of rigor fibers between cross-bridges and other structures, we studied the dependence of the rigor stiffness on the sarcomere length.

Initially, the stiffness of a fiber segment in the rigor state at a sarcomere length with full filament overlap was determined, and the fiber was transferred to relaxing solution. Stiffness in the relaxing solution (resting stiffness) was also determined at the sarcomere length. After stretching the fiber slightly to set a new sarcomere length, we transferred the fiber from the relaxing solution to rigor solution. Rigor stiffness at the new sarcomere length was determined. By repeating the same procedure, we determined both rigor and resting stiffness at various sarcomere lengths. Because the rigor stiffness of a fiber segment below the sarcomere length of 2.4 μm (and above 2.1 μm) retained a constant value, the resting and rigor stiffness values at other sarcomere lengths of the fiber were normalized with the rigor stiffness at full overlap. Fig. 6 summarizes the results.

Below the sarcomere length of 2.7 μm in relaxing solution, no resting stiffness was observed, but above this sarcomere length, resting stiffness became prominent. Above the sarcomere length of 3.0 μm, the resting stiffness took a constant value. The same resting stiffness was retained even at sarcomere lengths far beyond the end of the filament overlap (Fig. 6). This fact indicates that a large part of the resting stiffness originates from some parallel elastic components rather than the interaction between cross-bridges and thin filaments in relaxed fibers.

Rigor stiffness was constant at the sarcomere lengths between 2.1 and 2.4 μm. Above the sarcomere length of 2.4 μm, the rigor stiffness began to decrease with the decrease of the overlap between thick and thin filaments (Fig. 6). Finally, it reached the level of resting stiffness at the sarcomere length of 4.6 μm, suggesting that the elastic property of the parallel elastic components in rigor solution is the same as in relaxing solution. Thus, the resting stiffness was subtracted from the rigor stiffness at each measurement point and the corrected value of rigor stiffness was replotted in Fig. 6. (●). The slope of the corrected rigor stiffness above the sarcomere length of 2.4 μm is fairly linear.

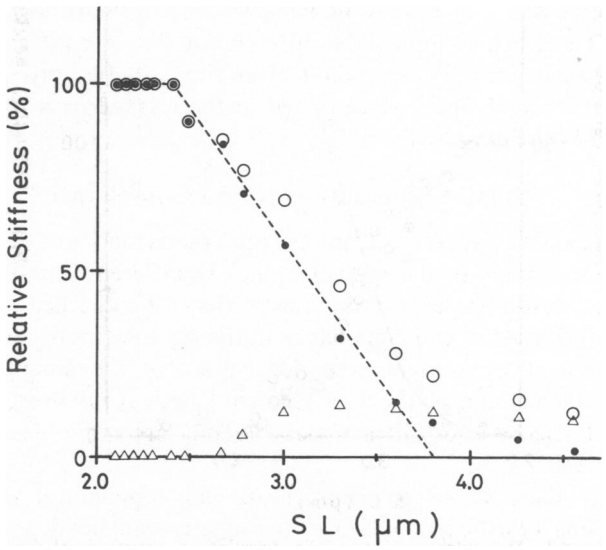

FIGURE 6 Dependence of rigor and resting stiffness of a single fiber segment on the sarcomere length. ○, rigor stiffness; △, resting stiffness; ● = ○ − △ at the sarcomere length of each measurement. The initial length of the fiber segment was 0.30 cm. The length of the segment at a new sarcomere length after stretch was measured and found to be the same as (initial segment length) × (the new sarcomere length)/(the initial sarcomere length). Broken line, assumed filament overlap (see Discussion). 13°C.

Dependence of Isometric Active Tension on the Sarcomere Length

We measured active tension development by glycerinated rabbit psoas fibers at various sarcomere lengths to compare it with the dependence of rigor stiffness on the sarcomere length. Since, in the time-course of the tension development by the fiber, such "creep" as that observed with active intact frog fibers (particularly at long sarcomere) (Gordon et al., 1966; Ter Keurs et al., 1978) was not observed, the final steady value of active tension was measured at every sarcomere length. The sarcomere length was determined by laser diffraction during measurements of the active tension. Resting tension at each sarcomere length was also measured in relaxing solution. Fig. 7 summarizes the results. The corrected rigor stiffness in Fig. 6 was replotted in Fig. 7. The relative active tension appears to scale with the corrected rigor stiffness.

Fig. 7 shows that the resting tension is small below the sarcomere length of 2.6 μm, but above this sarcomere length, the resting tension begins to increase more steeply with the increase of the sarcomere length, in correspondence with the appearance of resting stiffness at the sarcomere length of 2.7 μm in Fig. 6. The resting tension is relatively large in glycerinated rabbit psoas fibers. The resting tension, which is greater at longer sarcomere lengths, may stabilize the sarcomere length homogeneity upon activation, as is evident from the crisp laser diffraction pattern from activated glycerinated rabbit psoas fibers.

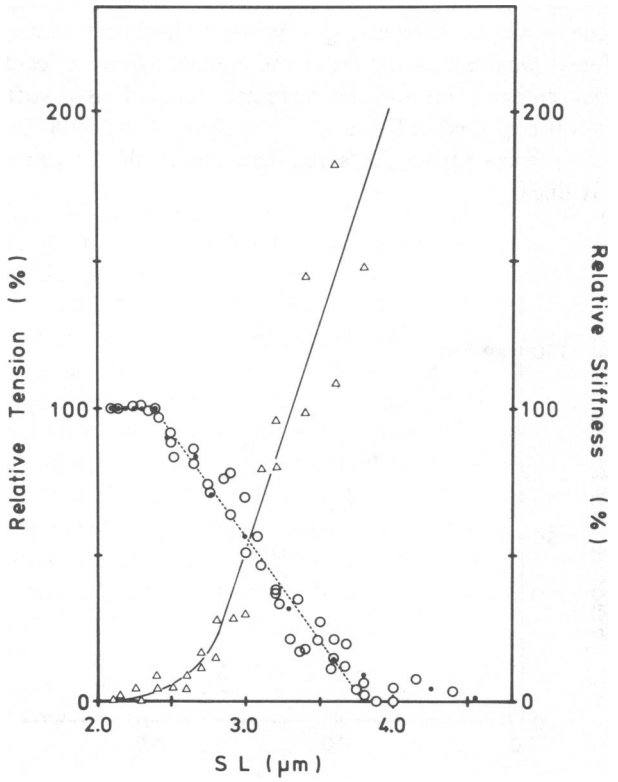

FIGURE 7 Dependence of active (○) and resting (△) tension development on the sarcomere length. The data were collected from two segments of single fiber and one segment of bundle of two fibers. The initial length of the fiber segments was 0.24–0.27 cm. 14°C. The tension values were normalized with the active tension at full overlap sarcomere length. The sarcomere length was determined from the diffraction pattern from a laser while muscle fibers were developing steady isometric tension. Broken line, assumed filament overlap (see Discussion). Corrected rigor stiffness (●) was replotted from Fig. 6.

DISCUSSION

Cross-Bridge Compliance in Rigor Fiber

The main findings of our work are (*a*) that the rigor stiffness is constant at sarcomere lengths between 2.1 and 2.4 μm, and (*b*) that the slope of the corrected rigor stiffness above the sarcomere length of 2.4 μm is fairly linear. A similar relation to sarcomere length was found with the isometric active tension of the same preparation. These findings support the idea that the rigor stiffness that we have measured resides in the cross-bridges as will be discussed below. The relation of the isometric active tension to the sarcomere length in glycerinated rabbit psoas fibers studied by Brenner (1980) also shows a break point at a sarcomere length near 2.4 μm.

Ford et al. (1981) studied the "instantaneous" stiffness in active intact frog fibers. By analyzing the dependence of the stiffness on the sarcomere length, they determined the distribution of the sarcomere compliance between cross-bridges and other structures such as thick filaments, thin filaments, and Z-line (see their Appendix A). Their analysis showed that most of the compliance in active frog muscle fibers originates in the cross-bridges.

We applied their analysis method to the rigor stiffness, assuming that the overlap between thick and thin filaments in rabbit psoas fibers begins at the sarcomere length of 2.36 μm and ends at the sarcomere length of 3.76 μm. These values were obtained from measurements showing that rabbit thin filaments are longer than frog thin filaments by 2×40 nm (Page and Huxley, 1963; Ebashi et al., 1969), and that the length of rabbit thick filaments is the same as that of frog thick filaments (Huxley, 1963; Trinick and Elliott, 1979). The theoretical overlap is shown by the broken line in Figs. 6 and 7. The corrected rigor stiffness nicely scales with the overlap.

Fig. 8 shows the relation to the sarcomere length of the muscle compliance multiplied by the overlap between thick and thin filaments. The compliance was obtained from the stiffness (Fig. 6 [●]). Theoretically (see Appendix A in Ford et al., 1981 and Appendix B in this article), the calculated points will be on the horizontal solid line, if 100% of the sarcomere compliance is the cross-bridge compliance and if there is no contribution of end compliance. The effect of end compliance to the plot in Fig. 8 is analyzed in Appendix B. Our experimental points are close to the broken line. As shown in Appendix B, this means that most (probably >80%) of the sarcomere compliance

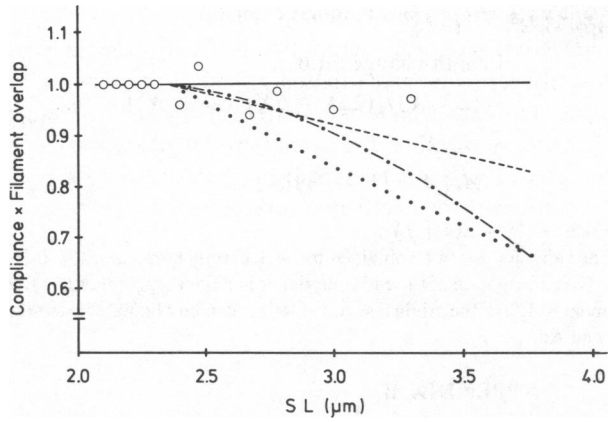

FIGURE 8 The relation of the relative compliance × filament overlap to the sarcomere length. The compliance was obtained from the stiffness shown by the closed circle in Fig. 6. See Appendix B for the explanation of the lines.

at full overlap in rigor fibers is the cross-bridge compliance.

Relations to Other Studies

Oosawa and his coworkers showed that the bending flexibility of thin filaments (F-actin–tropomyosin–troponin system) is increased by Ca^{++} and the flexibility of thin filaments decorated with heavy meromyosin is much more increased by Ca^{++} (Oosawa, 1977). Thin filaments in rigor fibers seem to be relatively rigid as discussed above. However, if the flexibility of thin filaments is assumed to contribute to the rigor stiffness (Fujime et al., 1979), the rigor stiffness will be smaller in the presence of Ca^{++} than in its absence. However, this was not the case as shown in our work. Thus, the bending flexibility of thin filaments in the overlapped and nonoverlapped regions has no significant contribution to the rigor stiffness.

The Young's modulus of the rigor stiffness at full overlap was 2.5×10^2 kg/cm^2. If a correction is made for the contribution of end compliance, the true rigor stiffness may become 3×10^2 kg/cm^2. This is ~40% of the Young's modulus obtained with active intact frog fibers by Ford et al. (1977).

The relatively low value of the Young's modulus of glycerinated rabbit psoas fibers in rigor is not due to denaturation of myosin in the fibers during glycerination; we found that fresh "chemically skinned" psoas fibers before glycerination gave the same stiffness. The low value is not due to the 3-ms step (up to 1% muscle length in our study); it has been found that the rigor stiffness does not increase greatly as speed of stretch is increased from 1.5 to 0.15 ms for a 0.5% muscle-length change (M. Schoenberg, personal communication). The value of the rigor stiffness obtained by Schoenberg et al. (1983) is also very close to our value. Thus, the difference of the stiffness may be due to the swelling of skinned fibers, the differences in animals, or the difference in state (rigor vs. contraction).

In that most of myosin heads form bonds with actin in rigor fibers of rabbit (Cooke and Franks, 1980; Lovell and Harrington, 1981), as well as of frog (Lovell et al., 1981), and fewer myosin heads form bonds with actin in active intact fibers (Haselgrove and Huxley, 1973; Matsubara et al., 1975), the true difference of the stiffness per a cross-bridge will be larger if the same value for the cross-bridge concentration in these two preparations is assumed.

Güth and Kuhn (1978) measured the "instantaneous" stiffness of active fibers and the rigor stiffness, using glycerinated rabbit psoas fibers. The Young's modulus of the rigor stiffness was slightly larger than that of the instantaneous stiffness, and $\sim 2 \times 10^2$ kg/cm^2, which is close to our value. The Young's modulus of the rigor stiffness obtained by Yamamoto and Herzig (1978) with skinned frog fibers is $\sim 6 \times 10^2$ kg/cm^2, if the rigor tension in their case is taken to be 30 N/cm^2 ($\simeq 3$ kg/cm^2), and is about two times larger than our value. Thus, it is more likely that the difference between our rigor stiffness and the "instantaneous" stiffness of active frog fibers by Ford et al. (1977) is due to differences in animals.

A similar study was made by Goldman and Simmons (1977), using skinned frog fibers. They found that the instantaneous stiffness of active muscle is 75% of rigor stiffness. Because they do not give the absolute values of fiber diameter in their paper, we cannot compare our value with theirs.

Conclusion

In summary, the compliance of rigor fibers mostly originates in the cross-bridges. Inasmuch as the nature of the cross-bridge compliance in rigor fiber is not the "rocking" of the SI head bound to thin filaments (Naylor and Podolsky, 1981; Cooke, 1981), the compliance could be due to a shape change in SI (possibly near the joint between SI and SII in view of no change in the angle of SI binding), or in SII as assumed by Huxley and Simmons (1971). The measurement of rigor stiffness is useful for discriminating these two possibilities (see Kimura and Tawada, 1984), because chemical modification techniques can be more easily applied to rigor fibers than to active fibers and because of the ease of stiffness measurement.

APPENDIX A

Estimation of End Compliance in a Muscle Segment from the Dependence of the Young's Modulus on the Segment Length

In this Appendix, we consider segments of muscle fiber with a given filament overlap.

The Young's modulus of a muscle segment is given by

$$E = (\Delta F/S)/(\Delta L/L), \qquad \text{(A1)}$$

where L is the segment length; S, the cross-sectional area; ΔL, the applied stretch length; ΔF, the tension increment generated by the stretch. Fig. 3

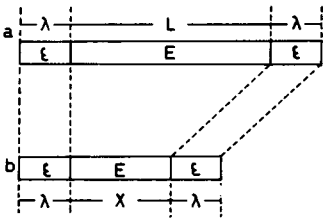

FIGURE 9 Model of the end compliance distribution in a muscle segment. (*a*) Fiber segment of the length of $2\lambda + L$. (*b*) Fiber segment after the length reduction to $1/n$ of the original length. The cross-sectional area is assumed to be the same throughout the entire length of the segments. E and ϵ are the Young's moduli of elasticity.

shows that glycerinated rabbit psoas fibers in rigor behave as a spring of linear compliance. Thus, E is constant.

If the compliance of a muscle segment is uniform along the fiber, E is independent of the segment length at a fixed sarcomere length. On the contrary, if the compliance of a muscle fiber segment near the tying knots at both ends is different from the true compliance of the muscle, E will depend on the segment length at a fixed sarcomere length. From the length dependence of the Young's modulus, we can evaluate the contribution of the end compliance.

For analysis, we assume a model for a muscle fiber segment comprising the end compliance as depicted in Fig. 9. The model assumes that a muscle fiber segment consists of three portions: two end-compliance portions and a true-compliance portion. The model also assumes (*a*) a constant length (λ) for the end-compliance portion, (*b*) a constant Young's modulus (ϵ) for the end compliance, (*c*) a constant Young's modulus (E) for the true compliance of the muscle, and (*d*) that both the end compliance and the true compliance are linear. The apparent Young's modulus of a muscle fiber segment comprising the end compliance is given by

$$E_o = E\epsilon(2\lambda + L)/(2\lambda E + L\epsilon), \tag{A2}$$

where the length of the muscle segment is $2\lambda + L$.

The apparent Young's modulus of the muscle fiber after $1/n$ reduction of the length is given by

$$\begin{aligned} E_{os} &= E\epsilon(2\lambda + X)/(2\lambda E + X\epsilon) \\ &= E\epsilon(2\lambda + L)/[\epsilon(2\lambda + L) + 2\lambda(E - \epsilon)n], \end{aligned} \tag{A3}$$

where the length of the shorter muscle segment is $2\lambda + X$ and $X = (2\lambda - 2\lambda n + L)/n$.

From Eqs. A2 and A3,

$$E_o/E_{os} = A + (1 - A)n, \tag{A4}$$

where $A = \epsilon(2\lambda + L)/(2\lambda E + L\epsilon)$.

The ratio of the length change in the true-compliance portion to the length change applied at one end of a muscle fiber segment is given by

$$\begin{aligned} &\text{Length-change ratio} \\ &= (\Delta L/L)/[(2\Delta\lambda + \Delta L)/(2\lambda + L)] \\ &= E_o/E \\ &= \epsilon(2\lambda + L)/(2\lambda E + L\epsilon) \\ &= A. \end{aligned} \tag{A5}$$

For a fiber segment of $1/n$ of the original length,

$$\begin{aligned} &\text{Length-change ratio} \\ &= (\Delta X/X)/[(2\Delta\lambda + \Delta X)/(2\lambda + X)] \\ &= E_{os}/E \\ &= A/[A + (1 - A)n], \end{aligned} \tag{A6}$$

where $X = (2\lambda - 2\lambda n + L)/n$.

The value for A can be obtained by back extrapolation of n to 0 in Eq. A4. The contribution of the end compliance in a fiber segment or in a fiber segment of $1/n$ of the original segment length can be calculated from Eqs. A5 and A6.

APPENDIX B

Contribution of End Compliance to the Plot of Compliance x Filament Overlap vs. Sarcomere Length

In Appendix A, we considered the case that the length of fiber segments was varied while keeping a constant sarcomere length. Here we consider the case that the length of fiber segments is varied by changing the sarcomere length (while the segments are in relaxing solution).

In this Appendix, we use the following notations for the compliance distribution in a fiber segment in rigor such as shown in Fig. 9:

C_e compliance in the entire λ portion (end compliance)

C_s compliance in the entire L portion (sarcomere compliance).

The compliance in the entire fiber segment is

$$C_f = 2C_e + C_s. \tag{B1}$$

The ratio of the length change in the true-compliance portion to the length change applied at one end of a muscle fiber segment is given as

$$\begin{aligned} &\text{Length-change ratio} \\ &= (C_s/L)/[(2C_e + C_s)/(2\lambda + L)] \\ &= (2\lambda/L + 1)/(2C_e/C_s + 1) \\ &= A. \end{aligned} \tag{B2}$$

Eq. B2 corresponds to Eq. A5. From Eq. B2,

$$2C_e/C_s = (2\lambda/L + 1)/A - 1. \tag{B3}$$

We may assume that $2\lambda/L \ll 1$. We also assume that

$$A = 1 - 0.2\phi \quad (1 \geq \phi \geq 0)$$

because the length-change ratio (A) appears to be a decreasing function of the filament overlap (ϕ) as shown in Results. Then, Eq. B3 becomes

$$\begin{aligned} 2C_e/C_s &= 1/A - 1 \\ &= 1/(1 - 0.2\phi) - 1 \\ &\simeq 0.2\phi. \end{aligned} \tag{B4}$$

C_s is a function of the filament overlap (see Appendix A in Ford et al., 1981). If we assume that the sarcomere compliance originates only in the cross-bridges,

$$C_s = C_c/\phi, \tag{B5}$$

where C_c is a constant. Eqs. B4 and B5 lead to

$$2C_e = 0.2C_c. \tag{B6}$$

From Eqs. B1, B5, and B6,

$$C_f\phi = (0.2\phi + 1)C_c. \quad \text{(B7)}$$

The normalized Eq. B7 is shown as a function of the sarcomere length by the broken line in Fig. 8. Eq. B7 nicely fits the experimental points. The broken line stands for the case that the sarcomere compliance in the L portion is only the cross-bridge compliance and the length-change ratio is 0.80 at a full overlap sarcomere due to the end compliance. If there is no contribution of the end compliance, $C_e = 0$. Then, from Eqs. B1 and B5,

$$C_f\phi = C_c = \text{constant}. \quad \text{(B8)}$$

Eq. B8 is shown by the solid line in Fig. 8.

If the Z-line together with the cross-bridges contributes to the sarcomere compliance,

$$C_s = C_z + C_c/\phi \quad \text{(B9)}$$

where C_z is the Z-line compliance.

Eqs. B1, B4, and B9 lead to

$$C_f\phi = 0.2\phi^2C_z + (C_z + 0.2C_c)\phi + C_c. \quad \text{(B10)}$$

Assuming $C_z/(C_z + C_c) = 0.2$, i.e., the Z-line contributes 20% of the sarcomere compliance with 80% contribution of cross-bridges at full overlap, Eq. B10 was calculated and is shown in Fig. 8 (dots).

If thick filaments together with cross-bridges contribute to the sarcomere compliance,

$$C_s = C_{mf}(2.4 - 1.4\phi) + C_c/\phi, \quad \text{(B11)}$$

where $C_{mf}(2.4 - 1.4\phi)$ is the thick-filament compliance (see Eq. A10 in Appendix A of Ford et al., 1981). Eqs. B1, B4, and B11 lead to

$$C_f\phi = -0.28\phi^3C_{mf} - 0.92\phi^2C_{mf} + (2.4C_{mf} + 0.2C_c)\phi + C_c. \quad \text{(B12)}$$

Assuming $C_{mf}/(C_{mf} + C_c) = 0.2$, i.e., thick filaments contribute 20% of the sarcomere compliance with 80% cross-bridge contribution at full overlap, Eq. B12 was calculated and is shown in Fig. 8 (dots and dashes).

If thin filaments together with cross-bridges contribute to the sarcomere compliance,

$$C_s = C_a(1.76 - 0.76\phi) + C_c/\phi, \quad \text{(B13)}$$

where $C_a(1.67 - 0.67\phi)$ is the thin-filament compliance (see Eq. A10 in Appendix A of Ford et al., 1981). Eqs. B1, B4, and B13 lead to

$$C_f\phi = -0.152\phi^3C_a - 0.408\phi^2C_a + (1.76C_a + 0.2C_c)\phi + C_c. \quad \text{(B14)}$$

Assuming $C_a/(C_a + C_c) = 0.2$, i.e., thin filaments contribute 20% of the sarcomere compliance with 80% cross-bridge contribution at full overlap, Eq. B14 was calculated. The calculated line (not shown) would be between the two lines of Eqs. B10 and B12 in Fig. 8.

Below the sarcomere length of 2.36 μm, the extent of filament overlap is constant while the sarcomere length is varied. Thus, the dependence of the end-compliance contribution on the muscle segment length discussed in Appendix A should be taken into account. However, since the length change of a fiber segment when the sarcomere length is reduced from 2.36 to 2.1 μm is small (~10%), we may assume that the end-compliance contribution is constant in the range of sarcomere lengths from 2.36 to 2.1 μm. Under this assumption, we calculated $C_f \times \phi$ below the sarcomere length of 2.36 μm by using Eqs. B1 and B4 and Eq. B13 with the second term on the righthand side replaced with C_c, and also assuming $C_a/(C_a + C_c) = 0.2$. The calculated values (relative) were 0.97 at 2.10 μm, 0.98 at 2.15 μm, 0.99 at 2.22 μm, and 1 at 2.36 μm of sarcomere lengths. These calculated values are slightly below the experimental points in Fig. 8. Since the standard deviation of the stiffness measurements with a single fiber segment in rigor at full overlap is about 2% ($N = 3$), the difference between the calculated and experimental values may be within experimental errors.

Fig. 8 shows that 20% contribution of the Z-line to the sarcomere compliance at full overlap clearly produces deviation of the line of the compliance × (filament overlap) plot from the experimental points. The deviation would be still visible even with 10% contribution of Z-line. Thus, the contribution of Z-line to the sarcomere compliance appears to be very small. A 20% contribution of thick or thin filaments to the sarcomere compliance at full overlap does not produce significant deviation of the line of the plot from the experimental points except at sarcomere lengths >3.0 μm. However, the deviation would be appreciably larger when >30% contribution of thick or thin filaments at full overlap is assumed. Thus, most (probably >80%) of the sarcomere compliance in rigor fibers at full overlap appears to be the cross-bridge compliance.

We would like to thank Dr. M. Schoenberg for critically reading the manuscript, and Dr. R. J. Podolsky and Dr. E. Eisenberg for invaluable comments on the work.

This work was supported by the Grant-in-Aid for Scientific Research No. 548377 from the Ministry of Education, Science and Culture of Japan to Dr. Tawada.

Received for publication 30 August 1982 and in final form 6 September 1983.

REFERENCES

Brenner, B. 1980. Effect of free sarcoplasmic Ca^{++} concentration on maximum unloaded shortening velocity: measurements on single glycerinated rabbit psoas muscle fibers. *J. Muscle Res. Cell Mot.* 1:409–428.

Brenner, B., M. Schoenberg, J. M. Chalovich, L. E. Green, and E. Eisenberg. 1982. Evidence for cross-bridge attachment in relaxed muscle at low ionic strength. *Proc. Natl. Acad. Sci. USA.* 79:7288–7291.

Civan, M. M., and R. J. Podolsky. 1966. Contraction kinetics of striated muscle fibers following quick changes in load. *J. Physiol. (Lond.)* 184:511–534.

Cooke, R., and K. Franks. 1980. All myosin heads form bonds with actin in rigor rabbit skeletal muscle. *Biochemistry.* 19:2265–2269.

Cooke, R. 1981. Stress does not alter the conformation of a domain of the myosin cross-bridge in rigor muscle fibers. *Nature (Lond.).* 294:570–571.

Delay, M. J., D. V. Vassallo, T. Iwazumi, and G. H. Pollack. 1979. Fast response of cardiac muscle to quick length change. *In* Cross-bridge Mechanism in Muscle Contraction. H. Sugi and G. H. Pollack, editors. University of Tokyo Press, Tokyo. 71–83.

Eastwood, A. B., D. S. Wood, K. L. Bock, and M. M. Sorenson. 1979. Chemically skinned mammalian skeletal muscle. 1. The structure of skinned rabbit psoas. *Tissue Cell.* 11:553–566.

Ebashi, S., M. Endo, and I. Ohtsuki. 1969. Control of muscle contraction. *Q. Rev. Biophys.* 2:351–384.

Eisenberg, E., and T. L. Hill. 1978. A cross-bridge model of muscle contraction. *Prog. Biophys. Molec. Biol.* 33:55–82.

Ford, L. E., A. F. Huxley, and R. M. Simmons. 1977. Tension responses to sudden length change in stimulated frog muscle fibers near slack length. *J. Physiol. (Lond.)* 269:442–515.

Ford, L. E., A. F. Huxley, and R. M. Simmons. 1981. The relation between stiffness and filament overlap in stimulated frog muscle fibers. *J. Physiol. (Lond.).* 311:219–249.

Fujime, S., S. Yoshino, and Y. Umazume. 1979. Optical diffraction study

on the dynamics of thin filaments in skinned muscle fibers. *In* Cross-bridge Mechanism in Muscle Contraction. H. Sugi and G. H. Pollack, editors. University of Tokyo Press, Tokyo. 51–67.

Goldman, Y. E., and R. M. Simmons. 1977. Active and rigor muscle stiffness. *J. Physiol. (Lond.).* 269:55–57p.

Gordon, A. M., A. F. Huxley, and F. J. Julian. 1966. Tension development in highly stretched vertebrate muscle fibers. *J. Physiol. (Lond.).* 184:143–169.

Gulati, J., and R. J. Podolsky. 1978. Contraction transients of skinned muscle fiber: Effect of calcium and ionic strength. *J. Gen. Physiol.* 72:701–716.

Güth, K., and H. J. Kuhn. 1978. Stiffness and tension during and after sudden length changes of glycerinated rabbit psoas muscle fibers. *Biophys. Struct. Mech.* 4:223–236.

Haselgrove, J. C., and H. E. Huxley. 1973. X-ray evidence for radial cross-bridge movement and for the sliding filament model in actively contracting skeletal muscle. *J. Mol. Biol.* 77:549–568.

Huxley, A. F. 1957. Muscle structure and theories of contraction. *Prog. Biophys. Biophys. Chem.* 7:255–318.

Huxley, A. F., and R. M. Simmons. 1970. A quick phase in the series-elastic component of striated muscle, demonstrated in isolated fibers from the frog. *J. Physiol. (Lond.).* 208:52–53p.

Huxley, A. F., and R. M. Simmons. 1971. Proposed mechanism of force generation in striated muscle. *Nature (Lond.).* 233:533–538.

Huxley, A. F. 1974. Muscular contraction (review lecture). *J. Physiol. (Lond.).* 243:1–43.

Huxley, H. E. 1963. Electron microscope studies on the structure of natural and synthetic protein filaments from striated muscle. *J. Mol. Biol.* 7:281–308.

Huxley, H. E. 1969. The mechanism of muscular contraction. *Sciences (N. Y.)* 164:1356–1366.

Kawai, M., and P. W. Brandt. 1976. Two rigor states in skinned crayfish single muscle fibers. *J. Gen. Physiol.* 68:267–280.

Kimura, M., and K. Tawada. 1984. Is the SII portion of the cross-bridge in glycerinated rabbit psoas fibers in rigor compliant? *Biophys. J.* 45:603–610.

Lovell, S. J., and W. F. Harrington. 1981. Measurement of fraction of myosin heads bound to actin in rabbit skeletal myofibrils in rigor. *J. Mol. Biol.* 149:659–674.

Lovell, S. J., P. J. Knight, and W. F. Harrington. 1981. Fractions of myosin heads bound to thin filaments in rigor fibrils from insect flight and vertebrate muscles. *Nature (Lond.).* 293:664–666.

Matsubara, I., N. Yagi, and H. Hashizume. 1975. Use of X-ray television for diffraction of the frog striated muscle. *Nature (Lond.).* 255:728–729.

Naylor, G. R. S., and R. J. Podolsky. 1981. X-ray diffraction of strained muscle fibers in rigor. *Proc. Natl. Acad. Sci. USA.* 78:5559–5563.

Oosawa, F. 1977. Actin-actin bond strength and the conformational change of F-actin. *Biorheology.* 14:11–19.

Page, S. G., and H. E. Huxley. 1963. Filament length in striated muscle. *J. Cell. Biol.* 19:369–390.

Schoenberg, M., B. Brenner, J. M. Chalovich, L. E. Green, and E. Eisenberg. 1983. Cross-bridge attachment in relaxed muscle. *In* Contractile Mechanisms in Muscle. G. H. Pollack and H. Sugi, editors. Plenum Press, New York. In press.

Tawada, K., and M. Kimura. 1983. Cross-linking studies related to the location of the rigor compliance in glycerinated psoas fibers: Is the SII portion of the cross-bridge compliant? *In* Contractile Mechanisms in Muscle. G. H. Pollack and H. Sugi, editors. Plenum Press, New York. In press.

Ter Keurs, H. E. D. J., T. Iwazumi, and G. H. Pollack. 1978. The sarcomere length-tension relation in skeletal muscle. *J. Gen. Physiol.* 72:565–592.

Trinick, J., and A. Elliott. 1979. Electron microscope studies of thick filaments from vertebrate skeletal muscle. *J. Mol. Biol.* 131:133–136.

Yamamoto, T., and J. W. Herzig. 1978. Series elastic properties of skinned muscle fibers in contraction and rigor. Pflügers Arch. 373:21–24.